

1  
2  
3  
4  
5  
6  
7  
8  
9  
10  
11  
12  
13  
14  
15  
16  
17  
18  
19  
20  
21  
22  
23  
24  
25  
26  
27  
28  
29  
30  
31  
32  
33  
34  
35  
36  
37  
38  
39  
40  
41  
42  
43  
44  
45  
46  
47  
48  
49  
50  
51  
52  
53  
54  
55  
56  
57  
58  
59  
60  
61  
62  
63  
64  
65

# 1 On the significance of the climate-dataset recording interval in characterising wind-driven 2 rain and simultaneous wind pressure. Part I: Scalar approach

3 José M. Pérez-Bella<sup>a</sup>, Javier Domínguez-Hernández<sup>a,\*</sup>, Enrique Cano-Suñén<sup>a</sup>, Juan J. del Coz-Díaz<sup>b</sup>,  
4 Mar Alonso-Martínez<sup>b</sup>

5 <sup>a</sup> Department of Construction Engineering, Engineering and Architecture School, University of Zaragoza,  
6 María de Luna, s/n, 50018 Zaragoza, Spain.

7 <sup>b</sup> Department of Construction Engineering, University of Oviedo, Edificio Departamental Viesques nº 7,  
8 33204 Gijón, Spain.

## 9 Abstract

10 The joint action of wind-driven rain and wind pressure is the main cause of water penetration in building  
11 facades, which causes various habitability and durability problems. The most widespread characterisation  
12 of both climate factors is based on exposure indices calculated in free-field conditions from records of  
13 precipitation - wind velocity (scalar indices) and wind direction (directional indices). The time resolution  
14 of this climate dataset defines the calculation effort and the accuracy obtained, and average daily,  
15 monthly, or annual records are typical due to their greater availability. This paper investigates the  
16 influence of the recording interval on the accuracy of these scalar exposure indices (driving-rain index,  
17 hereafter aDRI, and driving-rain wind pressure, hereafter DRWP) by assessing the nature and magnitude  
18 of errors associated with each time resolution. For this purpose, 10-min, hourly, daily, monthly and  
19 annual meteorological data collected over 15 years in 6 Spanish weather stations at locations  
20 characterised by different environments and topography are analysed. In addition, relationships capable of  
21 adjusting indices of any time resolution to an accuracy similar to that reached through 10-min records are  
22 proposed. In general, the value of driving-rain wind pressure exhibits greater sensitivity than the driving-  
23 rain index at this time resolution, incorporating significant errors even with daily datasets. In turn, the use  
24 of monthly and annual records should be discarded, given their high uncertainty. The results demonstrate  
25 how the daily datasets for aDRI indices and hourly datasets for DRWP values are sufficient to  
26 characterise these exposures with errors of less than 11%.

## 27 Keywords

28 Wind-driven rain; Wind pressure; Building façades; Climatic data; Error

---

\* Corresponding author. Department of Construction Engineering, University of Zaragoza (UZ), María de Luna, s/n, 50018, Zaragoza, Spain. Tel.Fax: +34 976 76 21 00.  
E-mail address:javdom@unizar.es (Javier Domínguez-Hernández)

1  
2  
3  
4  
5  
6  
7  
8  
9  
10  
11  
12  
13  
14  
15  
16  
17  
18  
19  
20  
21  
22  
23  
24  
25  
26  
27  
28  
29  
30  
31  
32  
33  
34  
35  
36  
37  
38  
39  
40  
41  
42  
43  
44  
45  
46  
47  
48  
49  
50  
51  
52  
53  
54  
55  
56  
57  
58  
59  
60  
61  
62  
63  
64  
65

1   **1. Introduction**

2   Rainwater penetration into facade materials causes various durability problems, such as erosion,  
3   corrosion, frost attack, salt crystallisation, surface soiling and discoloration, loss of adherence,  
4   deformations, cracking, and falling materials [1-5]. It is also one of the main factors affecting the  
5   hygrothermal performance of the building, reducing its thermal insulation and increasing energy  
6   consumption and emission of air pollutants [6-8]. In addition, this moisture is associated with different  
7   health problems for the tenants [9].

8   The penetration of atmospheric water is produced by a combination of rainwater on the facade and the  
9   action exerted by the wind on this water supply. The rain diverted by wind action (wind-driven rain,  
10   hereafter WDR) and the simultaneous driving-rain wind pressure (DRWP) are thus the main climatic  
11   factors involved in the penetration process [10-12]. Determining both parameters is a necessary task to  
12   evaluate the characteristic exposure conditions in each site and thus to define facade designs that  
13   guarantee the necessary watertightness.

14   The most widespread and functional method for determining WDR exposure is based on semi-empirical  
15   approaches, establishing experimental adjustments from wind and precipitation data collected under free-  
16   field conditions [13-14]. Thus, it is possible to define "airfield" indices associated with each location (i.e.,  
17   relative to free-field conditions), which can subsequently be refined using empirical coefficients to  
18   represent the specific conditions of each facade (such as surroundings, topography, and geometry) [15-  
19   17].

20   The study of DRWP has received much less attention than WDR exposure, despite its crucial role in the  
21   penetration process (reflected in the standardised watertightness tests) [11, 18-21]. The few studies  
22   performed have used the Bernoulli equation to determine the DRWP value, considering only the wind  
23   velocity records concurrent with precipitation events [22-24].

1  
2  
3  
4  
5  
6  
7  
8  
9  
10  
11  
12  
13  
14  
15  
16  
17  
18  
19  
20  
21  
22  
23  
24  
25  
26  
27  
28  
29  
30  
31  
32  
33  
34  
35  
36  
37  
38  
39  
40  
41  
42  
43  
44  
45  
46  
47  
48  
49  
50  
51  
52  
53  
54  
55  
56  
57  
58  
59  
60  
61  
62  
63  
64  
65

1 These exposure indices can be scalar (representing the overall exposure value at the site) or directional by  
2 also evaluating wind direction data to determine the exposure on each possible facade orientation [15, 25-  
3 26]. The directional results provide more comprehensive information but also require a greater calculation  
4 effort and access to additional weather data, which are not always available.

5 In this sense, the recording interval of the climatic data constitutes another important limitation that  
6 decisively influences the accuracy of the exposure indices. The climate datasets conventionally used to  
7 characterise these exposures (daily, monthly and annual) are obtained as arithmetic averages of raw  
8 measurement data generally not available (collected every 1, 5, and 10 min). In turn, these raw data  
9 reflect the linearisation of the meteorological sensor outputs [27]. Thus, these arithmetic means are a  
10 source of co-occurrence and averaging errors (due to omitting the simultaneity of wind only with rainfall  
11 intervals and to the mathematical averaging of the raw data, respectively) [28-31].

12 Some studies have addressed the required time resolution of these datasets for WDR calculations based  
13 on computational fluid dynamics (CFD), focusing their efforts on proposing improved averaging  
14 techniques for the raw measurement data [29-30]. However, recent work has demonstrated that these  
15 improved techniques are not suitable to semi-empirical calculation methods [32]. Thus, a systematic  
16 approach that determines the errors associated with different recording intervals has not yet been  
17 developed for semi-empirical calculations of WDR exposure (much less for DRWP exposure).  
18 Consequently, there are currently no guidelines to evaluate the accuracy and uncertainty of multiple  
19 studies conducted using datasets with low time resolution.

20 This article develops an exhaustive task of analysis of 10-min records collected between 2001 and 2016 in  
21 6 meteorological stations in the northwest of Spain, obtaining airfield exposure indices of WDR and  
22 DRWP based on 10-min, hourly, daily, monthly and annual datasets. This analysis aims to reduce this  
23 lack of information, offering a broad perspective on the nature and magnitude of errors associated with  
24 each recording interval for locations with different characteristics. In addition, general adjustment  
25 relations between the indices calculated from each dataset of different time resolution are proposed. For

1  
2  
3 1 clarity and given the diverse climatic data involved, this study is divided into two distinct parts: the  
4  
5 2 significance of the recording interval on the scalar results (Part I) and on the directional results (Part II).  
6  
7  
8  
9 3

## 10 11 4 **2. Background**

12  
13  
14  
15 5 Characterisation of the WDR exposure at sites can be performed by means of experimental  
16  
17 6 measurements, CFD methods and semi-empirical correlations [15]. Experimental measurements are  
18  
19 7 costly and entail long periods of observation. In turn, CFD methods require a significant calculation effort  
20  
21 8 and high-quality input data adapted to each specific situation. Only semi-empirical methods allow a  
22  
23  
24 9 simple and functional characterisation of the exposure in a large number of sites, although their  
25  
26 10 thoroughness is inferior to the other methods.  
27  
28

29 11 These semi-empirical methods are based on the 'WDR relationship', which uses free-field climate records  
30  
31 12 generally gathered at most of the weather stations and empirically fitted coefficients [13, 33]. By  
32  
33 13 multiplying simultaneous records of wind velocity  $U$  (m/s) and precipitation intensity  $R_h$  ( $l/m^2$ ), this  
34  
35 14 relationship allows estimation of an airfield WDR value ( $l/m^2$ ), using the value  $\alpha$  (s/m) as a coefficient  
36  
37  
38 15 physically related to the terminal falling velocity of raindrops and that depends on the intensity of  
39  
40 16 precipitation at each time point [14, 34]. Standards such as ISO 15927-3 or ASHRAE 160P also  
41  
42  
43 17 incorporate dimensionless coefficients (grouped here under the designation  $F_{wall\ indices}$ ) to determine the  
44  
45 18 WDR exposure on each specific facade, considering its shape (e.g., height, cover, and geometry), the  
46  
47 19 terrain roughness, the topography of the surroundings and nearby obstructions (Eq. 1) [16-17]. To ensure  
48  
49 20 the representativeness of the results, the calculation should be performed by averaging at least 10 years of  
50  
51 21 climate data (as stated in ISO standard 15927-3).  
52  
53  
54  
55

$$56 \quad WDR = F_{wall\ indices} \cdot \alpha \cdot U \cdot R_h \quad (1)$$

57  
58  
59  
60  
61  
62  
63  
64  
65

1  
2  
3 1 By also incorporating simultaneous records of wind velocity  $D$  ( $^\circ$ ), it is possible to determine the  
4  
5 2 directional distribution of the exposure in each facade orientation  $\theta$  ( $^\circ$ ). For this, Eq. (1) would be  
6  
7 3 multiplied by  $\cos(D-\theta)$ , thus considering only the wind direction records when the analysed facade is in a  
8  
9 4 leeward position (cosine projection with positive value) [15-17, 25]. In this work, scalar indices are  
10  
11 5 referred to those exposure values that do not incorporate climate records of wind direction, thus providing  
12  
13 6 only global (non-directional) exposure information.

14  
15  
16  
17 7 Based on this WDR relationship, the annual driving-rain index ( $aDRI$ ) is the simplest and most  
18  
19 8 generalised indicator to evaluate the average annual exposure at each location [13, 26, 31, 35-38]. For its  
20  
21 9 scalar calculation, the coefficient  $\alpha$ , directional characterisation and wall indices (i.e., obtaining an  
22  
23 10 airfield index) are ignored. This gives an  $aDRI$  value ( $m^2/s$ ), which qualitatively characterises the scalar  
24  
25 11 exposure from the  $k$  records collected at the site over  $N$  years (see Eq. 2). In spite of its simplicity, this  
26  
27 12 index can be used as reference to obtain more refined results, incorporating adequate values for the  
28  
29 13 coefficient  $\alpha$  and the wall indices.

$$aDRI = \frac{\sum_{i=1}^k U_i \cdot \left( \frac{R_{hi}}{1000} \right)}{N} \quad (2)$$

30  
31  
32  
33  
34  
35  
36  
37  
38  
39  
40 14 On the other hand, the penetration of water into building facades does not depend exclusively on the  
41  
42 15 water supply provided by wind-driven rain. On the contrary, it depends strongly on the simultaneous  
43  
44 16 existence of wind pressure on the facade that is capable of overcoming the surface tension and capillary  
45  
46 17 pressure of the water contained in the material deficiencies. Thus, it is estimated that this is the most  
47  
48 18 sensitive parameter related to water penetration in facades without openings and pores greater than 1 mm  
49  
50 19 [11]. Therefore, characterising the  $DRWP$  exposure at the location is of equal interest to studying the  
51  
52 20 WDR.

53  
54  
55  
56  
57 21 The most widespread method of determining the value of  $DRWP$  (Pa) is based on the analysis of the  $m$   
58  
59 22 wind velocity records  $U$  (m/s), which are simultaneous to intervals with precipitation during the studied  
60  
61

1  
2  
3 1 period ( $m \leq k$ ). This is performed using the Bernoulli equation (Eq. 3), where  $C_p$  (-) represents the  
4  
5 2 pressure coefficient (usually equal to 1) and  $\rho_{air}$  the air density (generally set at  $1.2 \text{ kg/m}^3$ ). As in Eq. 2,  
6  
7 3 this result represents the scalar exposure associated with the site (in free-field conditions), and the factor  
8  
9 4  $\cos(D-\theta)$  can also be incorporated to obtain the directional distribution of the DRWP exposure.

$$DRWP = \frac{\sum_{i=1}^m C_p \cdot \frac{1}{2} \cdot \rho_{air} \cdot U_i^2}{m} \quad (3)$$

19 5 In both equations (Eqs. 2 and 3), it is possible to use climate data with different recording intervals and  
20  
21 6 therefore different time resolution, without there being uniformity in the studies developed so far [11, 15,  
22  
23 7 23-24, 26, 31, 35-38]. On the contrary, in each case, the available climate records (usually annual,  
24  
25 8 monthly or daily data) have been used. However, the selected recording interval influences the accuracy  
26  
27 9 of the results by incorporating two types of errors in the exposure indices: a co-occurrence error ( $e_1$ ),  
28  
29 10 which is due to not exhaustively recording the simultaneity of wind and precipitation events, and an  
30  
31 11 averaging error ( $e_2$ ), which is due to the smoothing of the values of the climatic variables when averaging  
32  
33 12 of the raw data [29-30].

34  
35  
36  
37  
38 13 To these errors other uncertainties must be added, which are associated with the collection of records  
39  
40 14 through the meteorological sensor outputs: small-scale variability of the atmosphere conditions, noise in  
41  
42 15 electronic devices, precipitation gauge errors, disturbances in wind measurements due to topographic  
43  
44 16 effects and random instrumental errors among others. These random uncertainties can be minimised by  
45  
46 17 collecting the sensor outputs as 2- to 10-min averages, recording wind data at 10 m above ground level in  
47  
48 18 an open field (free-field conditions), and using recording precipitation gauges with high resolution [27].  
49  
50 19 In this sense, the 10-min records ensure a good representation of the rapid variations that characterise  
51  
52 20 precipitation and wind phenomena [39-41].

53  
54  
55  
56  
57 21 Some works have proposed weighted averaging techniques for the raw measurement data, obtaining  
58  
59 22 climate datasets to calculate with less error the WDR exposure using CFD methods [29-30]. However, a

1  
2  
3  
4  
5  
6  
7  
8  
9  
10  
11  
12  
13  
14  
15  
16  
17  
18  
19  
20  
21  
22  
23  
24  
25  
26  
27  
28  
29  
30  
31  
32  
33  
34  
35  
36  
37  
38  
39  
40  
41  
42  
43  
44  
45  
46  
47  
48  
49  
50  
51  
52  
53  
54  
55  
56  
57  
58  
59  
60  
61  
62  
63  
64  
65

1 recent study has shown that these weighted techniques reduce the accuracy of semi-empirical calculations  
2 [32]. Assessing climate records collected over 6-12 months in 3 Canadian cities, this study also identified  
3 an average error close to 12% in the WDR airfield indices obtained from hourly datasets, compared to  
4 those calculated using 5- and 10-min records. However, the errors associated with other conventional  
5 intervals (daily, monthly, and annual) were not analysed, nor was the nature of the error ( $e_1$  and  $e_2$ )  
6 differentiated. Using 30 years of daily records in 80 Spanish locations, another study quantified the  $e_1$  and  
7  $e_2$  errors present in the monthly and annual airfield indices of WDR (with respect to their daily  
8 equivalents), concluding that both sources of error were equal and similar in the monthly and annual  
9 indices [31]. The same study was performed in 41 Greek cities, obtaining analogous results, although  
10 with a higher prevalence of averaging error [42].

11 All of these studies are partial approximations to the problem in which the climatic series are not very  
12 representative, or the analysis of the most conventional recording intervals is obviated, or the error with  
13 respect to recording intervals sufficiently exhaustive (e.g., 10-min records) is not identified. In addition,  
14 none of them analyses the effect of the time resolution of the dataset on the DRWP characterisation.  
15 Consequently, to the best of the authors' knowledge, a systematic study that comprehensively  
16 characterises the effect of the time resolution of the dataset on the accuracy of the semi-empirical airfield  
17 indices of both WDR and DRWP exposures has not yet been conducted.

18 Thus, guidelines to assess the real accuracy of the exposure results obtained from datasets of low time  
19 resolution are lacking. Given that these studies are the most common (due to the difficulty in accessing  
20 hourly data with the representativeness required by ISO 15927-3 and ASHRAE 160P standards), most of  
21 the published characterisations for both exposures have been performed without knowing their real  
22 uncertainty range [15, 35-38]. Similarly, although adjustment relationships have been defined between  
23 daily, monthly and annual exposure indices, extrapolations to achieve an accuracy similar to that of the  
24 indices based on raw measurement data have not yet been developed.

1  
2  
3  
4  
5  
6  
7  
8  
9  
10  
11  
12  
13  
14  
15  
16  
17  
18  
19  
20  
21  
22  
23  
24  
25  
26  
27  
28  
29  
30  
31  
32  
33  
34  
35  
36  
37  
38  
39  
40  
41  
42  
43  
44  
45  
46  
47  
48  
49  
50  
51  
52  
53  
54  
55  
56  
57  
58  
59  
60  
61  
62  
63  
64  
65

1 To clarify these issues, this paper analyses hourly, daily, monthly and annual climate records, identifying  
2 the nature and magnitude of the errors associated with each record interval in the scalar airfield indices  
3 defined by Eqs. 2 and 3. To compare and assess these errors, the exposure values calculated from 10-min  
4 records are taken as a reference. In addition, adjustment relationships to extrapolate results with an  
5 accuracy similar to that defined by 10-min records from the indices obtained through any time resolution  
6 of the dataset are proposed.

7

### 8 **3. Error assessment in the scalar characterisation of WDR and DRWP airfield indices**

#### 9 *3.1 Research scope*

10 The increasing deployment of automatic weather stations equipped with data-loggers capable of  
11 collecting and transmitting raw data in real time (or storing them until download) offers new possibilities  
12 to incorporate better-time-resolution records in the calculations previously described.

13 For this study, 6 automatic stations installed since 2000 in the northwest of Spain (Galicia region) have  
14 been selected. The choice of these stations is justified by the availability of sufficiently representative  
15 meteorological datasets, which has allowed the examination of 15 years of records in all of them (1 Feb.  
16 2001 – 31 Jan. 2016). At each station, more than 780,000 10-min intervals have been analysed, with  
17 simultaneous records of precipitation intensity and wind velocity (measured at 10 m above open flat  
18 ground). Less than 1.5% of the analysed intervals lack records, as a result of failures, problems with data  
19 transmission or storage, maintenance, etc., which guarantees the representativeness of the historical  
20 series. The reliability and longevity of these datasets ensure that the results obtained are not influenced by  
21 years of exceptional climatology nor by prolonged interruptions of the records.

22 The devices used to record these climatic variables conform to the guidelines set by the World  
23 Meteorological Organisation (see Fig. 1) and form part of the official meteorological network of the

1  
2  
3 1 region of Galicia [27, 43]. To obtain the dataset corresponding to other usual recording intervals (e.g.,  
4  
5 2 hourly, daily, monthly and annual), 10-min records have been arithmetically added and averaged using a  
6  
7 3 spreadsheet program.  
8  
9

10 4  
11  
12  
13  
14 5 **Fig. 1.** Characteristics and location of the 6 analysed weather stations.  
15  
16  
17 6

18  
19  
20 7 Bordered by the Atlantic Ocean on its northern and western boundaries (see Fig. 2), Galicia presents the  
21  
22 8 highest WDR and DRWP exposures in Spain, especially near the coast and the numerous ocean-drowned  
23  
24 9 river valleys [23, 24, 31]. The west coast and the interior of the region are characterised by a topography  
25  
26 10 of low hills and subject to strong winds from the Atlantic Ocean. It also has an oceanic climate with  
27  
28 11 dispersed precipitation throughout the year and seasonally more intense (in autumn and winter). In  
29  
30 12 northern and eastern Galicia, the more rugged topography (reaching elevations of up to 2,100 m near the  
31  
32 13 O Invernadeiro station) reduces the influence of the ocean on the local climate. This makes possible the  
33  
34 14 existence of a warm-summer Mediterranean climate, with more concentrated rainfall in autumn and  
35  
36 15 winter [44].  
37  
38  
39  
40  
41 16

42  
43  
44  
45 17 **Fig. 2.** Location of the 6 weather stations selected for the conducted study. *Darker colours represent*  
46 18 *higher elevations.*  
47  
48 19  
49  
50

51 20 In addition to this climatic variety and high exposure, the 6 stations are characterised by different  
52  
53 21 environmental conditions, elevation, topography and distance to the coast. Two of the stations correspond  
54  
55 22 to coastal locations (CIS Ferrol and Corrubedo) located less than 1 km from the ocean and at low  
56  
57 23 elevation. CIS Ferrol is also located in the important Ría de Ferrol (a wide ocean-drowned river valley),  
58  
59  
60  
61  
62  
63  
64  
65

1  
2  
3  
4  
5  
6  
7  
8  
9  
10  
11  
12  
13  
14  
15  
16  
17  
18  
19  
20  
21  
22  
23  
24  
25  
26  
27  
28  
29  
30  
31  
32  
33  
34  
35  
36  
37  
38  
39  
40  
41  
42  
43  
44  
45  
46  
47  
48  
49  
50  
51  
52  
53  
54  
55  
56  
57  
58  
59  
60  
61  
62  
63  
64  
65

1 bordered by low hills. The Pedro Murias station is located in the area of other small estuary denoted Ría  
2 de Ribadeo less than 4 km from the coast and on a flat terrain. Above 350 m of elevation, the stations of  
3 Queimadelos and Campus Lugo are located in wooded and urban environments, respectively. The last  
4 station is located at 1,026 m elevation, in the mountains of the interior belonging to the Natural Park O  
5 Invernadeiro.

6 The stations located close to the coast and subjected to strong ocean winds are highly exposed to wind  
7 (mean wind velocity of 4.09 m/s in Pedro Murias and 3.17 m/s in CIS Ferrol), whereas for stations  
8 located inland, only O Invernadeiro reaches 2.30 m/s (due to its higher elevation). The Queimadelos  
9 station, at 371 m and in a wooded environment, presents the lowest wind exposure (mean wind velocity  
10 of 1.37 m/s). There are also significant rainfall variations, ranging from 948 mm/year in Campus Lugo to  
11 1,785 mm/year in Queimadelos. The O Invernadeiro station, due to its altitude, also has a high rainfall  
12 (1,651 mm/year). Altogether, this variety of conditions guarantees the representativity and validity of the  
13 obtained results for different types of locations and exposure conditions.

### 15 *3.2 Calculations and results*

16 Using the climate datasets associated with different recording intervals, the scalar exposure indices  
17 described in Eqs. 2 and 3 have been calculated for each location. For clarity, each exposure index is  
18 prefixed with an acronym  $j$  to represent the recording interval used in its calculation (i.e., " $h$ " for hourly  
19 calculations, " $d$ " for daily, " $m$ " for monthly and " $a$ " for annual). Thus, the values used as reference (based  
20 on 10-min records) are denoted as  $10'aDRI$  and  $10'DRWP$ . These results are presented in Table 1.

22 **Table 1.**  
23 Exposure results to wind-driven rain and simultaneous wind pressure for climate datasets of different time  
24 resolution.

1  
2  
3  
4  
5  
6  
7  
8  
9  
10  
11  
12  
13  
14  
15  
16  
17  
18  
19  
20  
21  
22  
23  
24  
25  
26  
27  
28  
29  
30  
31  
32  
33  
34  
35  
36  
37  
38  
39  
40  
41  
42  
43  
44  
45  
46  
47  
48  
49  
50  
51  
52  
53  
54  
55  
56  
57  
58  
59  
60  
61  
62  
63  
64  
65

1  
2  
3  
4  
5  
6  
7  
8  
9  
10  
11  
12  
13  
14  
15  
16  
17  
18  
19  
20  
21  
22  
23  
24  
25  
26  
27  
28  
29  
30  
31  
32  
33  
34  
35  
36  
37  
38  
39  
40  
41  
42  
43  
44  
45  
46  
47  
48  
49  
50  
51  
52  
53  
54  
55  
56  
57  
58  
59  
60  
61  
62  
63  
64  
65

These exposure indices are consistent with those identified in 2014 by another study conducted in the region of Galicia, which produced two exposure isopleth maps from daily records collected at 80 stations [24]. Only Campus Lugo, with a value of 2.06 m<sup>2</sup>/s, slightly exceeds the range 0-2 m<sup>2</sup>/s indicated by the daDRI isopleth map for its area. Likewise, only the dDRWP value from O Invernadeiro (5.10 Pa), exceeds the range of 0-5 Pa marked by the isopleth exposure map for its zone. This consistency with previous results reinforces the validity of the values presented in Table 1.

However, the presented values show that the exposure calculated using datasets with a smaller recording interval (and that are therefore more accurate and realistic) is higher to that identified by the daDRI and dDRWP indices. It follows that the exposure characterisation provided by these exposure maps, like many others available in the bibliography and obtained from low-time-resolution records, need additional corrections to avoid underestimating the actual exposure in the sites. Quantifying the magnitude of these underestimates according to the recording interval used in the calculation is therefore a key factor to improve the accuracy of this type of study.

To analyse the nature of the errors associated with each time resolution  $j$ , the same previous calculation has been repeated (Eqs. 2 and 3), but those 10-min wind records corresponding to intervals without precipitation were removed from the hourly, daily, monthly and annual averages. The result eliminates the co-occurrence error, obtaining exposure indices in which only the averaging error  $e_2$  (see Table 2) appears. For clarity, the subscript  $e_2$  is incorporated into these refined exposure values (without co-occurrence error).

**Table 2.**  
Exposure results without co-occurrence error for climate datasets with different time resolutions.

1  
2  
3 1 The difference between the 10-min exposure values and the values thus refined for each recording  
4  
5 2 interval  $j$  allows characterising the characteristic averaging error at each time resolution ( $e_2$ ). The  $e_1$  error  
6  
7 3 can then be obtained as the difference between the total error (i.e.,  $e_1 + e_2$ ) and the error linked exclusively  
8  
9 4 to the mathematical averaging of the climate records,  $e_2$  (Eqs. 4-8). The results of this analysis are  
10  
11 5 presented in Table 3 (expressed as percentages).

$${}_{j}aDRI \text{ error } (e_1 + e_2) = \frac{100 \cdot ({}_{j}aDRI - 10' aDRI)}{10' aDRI} \quad (4)$$

$${}_{j}aDRI \text{ error } e_2 = \frac{100 \cdot ({}_{j}aDRI_{e_2} - 10' aDRI)}{10' aDRI} \quad (5)$$

$${}_{j}DRWP \text{ error } (e_1 + e_2) = \frac{100 \cdot ({}_{j}DRWP - 10' DRWP)}{10' DRWP} \quad (6)$$

$${}_{j}DRWP \text{ error } e_2 = \frac{100 \cdot ({}_{j}DRWP_{e_2} - 10' DRWP)}{10' DRWP} \quad (7)$$

$$\text{error } e_1 = \text{error}(e_1 + e_2) - \text{error } e_2 \quad (8)$$

6

7 **Table 3.**

8 Percentage errors derived from the non-co-occurrence of wind and rain ( $e_1$ ) and from the averaged data  
9 ( $e_2$ ) for climate datasets of different time resolution (regarding 10-min values).

10

11 As expected, the magnitude of the errors increases with decreasing time resolution of the climate dataset.  
12 However, this growth is not proportional to the recording interval, nor are the errors similar in both  
13 exposure indices for the same time resolution. Nor do the factors causing the error have the same  
14 influence on the different recording intervals (see Figs. 3 and 4). It is also observed that although both  $e_1$   
15 and  $e_2$  tend to underestimate the existing exposure, in the case of hourly datasets, both sources of error  
16 can counteract each other, thus reducing the resulting error.

1  
2  
3 1  
4  
5  
6 2 **Fig. 3.** Magnitude and nature of the aDRI error associated with each recording interval and its fluctuation  
7 3 for the different analysed locations.  
8

9 4  
10  
11  
12 5 **Fig. 4.** Magnitude and nature of the DRWP error associated with each recording interval and its  
13 6 fluctuation for the different analysed locations.  
14  
15

#### 16 7 17 18 19 8 **4. Discussion** 20

21  
22 9 By analysing the results presented in Table 1, it can be observed that the sites subjected to a greater mean  
23  
24 10 wind velocity also exhibit higher values of 10'DRWP exposure (see Fig. 1). This correlation is consistent  
25  
26 11 with the high coefficients of determination  $R^2$  identified between values of DRWP and wind pressure in  
27  
28 12 different countries [24, 26, 38]. However, site pluviometry is not a determining factor in estimating the  
29  
30 13 aDRI value, making a specific analysis of precipitation and simultaneous wind records to determine the  
31  
32 14 WDR exposure unavoidable.  
33

34  
35  
36  
37 15 The maximum values of WDR and DRWP exposure are identified at stations closest to the coast  
38  
39 16 (Corrubedo 7.98 m<sup>2</sup>/s and 40.82 Pa, respectively), thus presenting a greater risk of water penetration in  
40  
41 17 the facades. Pedro Murias and Queimadelos, somewhat further from the coast, have lower WDR  
42  
43 18 exposures than Corrubedo and CIS Ferrol. Campus Lugo, in an urban environment in the interior of  
44  
45 19 Galicia, exhibits the lowest aDRI value (2.23 m<sup>2</sup>/s). Despite its distance to the coast, O Invernadeiro  
46  
47 20 reaches a 10'aDRI value of 5.39 m<sup>2</sup>/s, due to its elevation and high rainfall. In contrast, its DRWP value is  
48  
49 21 lower than that of the coastal stations. In this sense, the lowest values of DRWP exposure occur in  
50  
51 22 stations characterised by their urban and forest environment: Campus Lugo (4.20 Pa) and Queimadelos  
52  
53 23 (3.57 Pa).  
54  
55  
56  
57  
58  
59  
60  
61  
62  
63  
64  
65

1  
2  
3  
4  
5  
6  
7  
8  
9  
10  
11  
12  
13  
14  
15  
16  
17  
18  
19  
20  
21  
22  
23  
24  
25  
26  
27  
28  
29  
30  
31  
32  
33  
34  
35  
36  
37  
38  
39  
40  
41  
42  
43  
44  
45  
46  
47  
48  
49  
50  
51  
52  
53  
54  
55  
56  
57  
58  
59  
60  
61  
62  
63  
64  
65

1 Considering the errors associated with each recording interval (Figs. 3-6), it is observed that the use of  
2 hourly datasets introduces an average error of 1.46% and 10.48% in the WDR and DRWP exposure  
3 values, respectively. In any case, the error varies between the analysed stations, depending on the  
4 particular characteristics of the atmospheric events at each site. Thus, the standard deviations  $\sigma$  for haDRI  
5 and hDRWP values reach 1.2% and 4.9%, respectively. In the case of daily datasets, the mean errors  
6 increase to 8.15% for the WDR values (still below the error associated with the hDRWP value) and  
7 37.62% for the dDRWP values. Similar to the hourly errors, the variability is also significant ( $\sigma$  is equal  
8 to 4.0% for the daDRI indices and 10.7% for the dDRWP indices).

9 For their part, the monthly and annual datasets introduce very high errors in the scalar characterisation of  
10 the exposure, without there being a significant difference in accuracy between both recording intervals.  
11 Thus, the mean error for the maDRI values reaches 28.87% ( $\sigma = 8.8%$ ) and is 31.83% for the aaDRI  
12 indices ( $\sigma = 10.6%$ ). In the case of DRWP exposure, the mean error of the mDRWP values reaches  
13 57.92% ( $\sigma = 10.1%$ ), and that of aDRWP values reaches 59.47% ( $\sigma = 9.9%$ ).

14 As observed, in general, the error associated with aDRI values is significantly less than that identified in  
15 the DRWP indices for the same recording interval. This fact can be explained by the different number of  
16 climatic variables involved in each exposure index, and by their variability during precipitation periods.  
17 In calculating the DRWP value, the magnitude of the error depends on the influence of the co-occurrence  
18 and averaging errors on a single variable (wind velocity). This meteorological dataset is highly variable,  
19 so it is especially sensitive to the averaging error. However, the aDRI index results from the product  
20 between this wind velocity dataset and the simultaneous precipitation data at each interval. This  
21 weighting reduces the sensitivity to the averaging error and also minimises the co-occurrence error: even  
22 if a wind velocity datum not simultaneous to precipitation is considered, its associated precipitation datum  
23 does not contribute to the precipitation interval, thus reducing the influence of this wind datum in the  
24 daDRI value calculation.

1  
2  
3 1 Thus, although the averaging error ( $e_2$ ) is a secondary source of error for calculating the WDR exposure,  
4  
5 2 it is clearly more influential than the co-occurrence error for the calculation of the DRWP exposure (Figs  
6  
7 3 5 and 6). Likewise, although co-occurrence errors ( $e_1$ ) exhibit a similar influence on both exposure  
8  
9 4 indices, this is slightly lower for the calculation of WDR exposure. For all of the above, the datasets used  
10  
11 5 to characterise the DRWP exposure require a better time resolution than those employed for aDRI  
12  
13 6 calculation if both characterisations are intended to have similar levels of uncertainty.  
14  
15  
16  
17 7  
18  
19  
20  
21 8 **Fig. 5.** Evolution of mean calculation errors in aDRI values for the usual recording intervals used for  
22 9 climate datasets (logarithmic scale).  
23  
24 10  
25  
26  
27 11 **Fig. 6.** Evolution of mean calculation errors in DRWP values for the usual recording intervals used for  
28 12 climate datasets (logarithmic scale).  
29  
30  
31 13  
32  
33  
34 14 In summary, it can be said that the error committed (and also its dispersion or standard deviation) grows  
35  
36 15 rapidly as the recording interval increases, stabilising for the monthly - annual interval. Based on the 10-  
37  
38 16 min results, only the hourly datasets provide estimates of DRWP exposure with errors less than 11%. In  
39  
40 17 the case of aDRI indices, only the hourly and daily datasets maintain an average error below this  
41  
42 18 threshold. The distinct recording interval required to calculate both exposures with a similar level of  
43  
44 19 accuracy is thus shown. Those climate datasets with lower time resolution (i.e., monthly and annual  
45  
46 20 datasets), although they significantly reduce the calculation effort, should be discarded owing to their high  
47  
48 21 uncertainty.  
49  
50  
51  
52  
53 22 The above suggests the need to perform a critical re-analysis of the WDR and DRWP characterisation  
54  
55 23 studies performed so far using climate datasets with low time resolution. Given the representativeness of  
56  
57 24 the study conditions (long series of records with less than 1.5% of missing data and locations with  
58  
59 25 different conditions), the obtained error ranges can serve as guidelines for this re-analysis, assessing the

1  
2  
3  
4  
5  
6  
7  
8  
9  
10  
11  
12  
13  
14  
15  
16  
17  
18  
19  
20  
21  
22  
23  
24  
25  
26  
27  
28  
29  
30  
31  
32  
33  
34  
35  
36  
37  
38  
39  
40  
41  
42  
43  
44  
45  
46  
47  
48  
49  
50  
51  
52  
53  
54  
55  
56  
57  
58  
59  
60  
61  
62  
63  
64  
65

1 uncertainty associated with the recording interval used in locations subject to different environmental  
2 conditions and exposure.

3

4 *4.1 Fitting relationships.*

5 In any case, climate datasets with exhaustive and simultaneous precipitation and wind velocity records are  
6 often unavailable in many regions (the number of suitable weather stations is often insufficient, or the  
7 records cover a non- representative number of years). Therefore, several studies have identified simple  
8 linear regressions that allow extrapolating scalar values of WDR exposure associated with different  
9 recording intervals [26, 31, 36-38, 42]. In this manner, the possibility of improving the accuracy of the  
10 results obtained from deficient data series (e.g., from aaDRI or maDRI values, up to its corresponding  
11 daDRI estimation) exists.

12 In general, there is a great coincidence between the aaDRI-maDRI adjustments identified in different  
13 geographic areas, such as Spain, Brazil, Chile, Greece, India and Nigeria, with coefficients of  
14 determination higher than 0.95 [38]. However, Figs. 5 and 6 show that the improvement provided by  
15 these adjustments is not significant because the monthly indices maintain very high uncertainties, similar  
16 to the annual ones.

17 This coincidence between different regions is also maintained in the maDRI-daDRI and aaDRI-daDRI  
18 relationships: Fig. 7 compiles the linear regressions obtained for different countries from the results of  
19 studies that have analysed daily climate datasets [26, 31, 38, 42]. As observed, the adjustments associated  
20 with the 6 sites of Galicia are similar to those of the whole of Spain, in addition to those of other areas in  
21 middle latitudes, such as Greece and much of Chile. Brazil, located in a tropical zone and influenced by  
22 monsoon-type precipitations, presents a more divergent adjustment. This suggests that these adjustment  
23 relationships are related to the pluviometric and eolian patterns of each region, being similar in areas with  
24 similar climatic conditions (generically, mid-latitudes with seasonal rainfall).

1  
2  
3 1  
4  
5  
6 2 **Fig. 7.** (a) Best-fit linear relationship between daDRI and maDRI; (b) best fit-linear relationship between  
7 3 daDRI and aaDRI, and its comparison with different countries.  
8 4  
9

10  
11 5 For all of the above, it is presumed that the good correlations between the indices aaDRI-maDRI-daDRI  
12 6 also extend to scalar exposure indices obtained by datasets with a shorter recording interval. Thus, Fig. 8  
13  
14 7 shows the simple linear regression between the 10-min indices of WDR exposure and those  
15  
16 8 corresponding to other recording intervals for the 6 stations analysed. In all cases, the strong correlation  
17  
18 9 exists, with coefficients of determination close to the unit (especially for haDRI-10'aDRI and daDRI-  
19  
20 10 10'aDRI adjustments).  
21  
22

23  
24  
25  
26 11 These relationships could be used in areas with a similar climate as a first approximation to estimate  
27  
28 12 accurate scalar indices of WDR exposure via low-time-resolution datasets. However, because no similar  
29  
30 13 studies have been developed in other geographical areas, their validity and reliability should still be  
31  
32 14 verified. It is up to subsequent studies to take on the challenge of analysing raw measurement data in  
33  
34 15 other regions, verifying and refining, if appropriate, the proposed extrapolations.  
35  
36  
37  
38 16

39  
40  
41 17 **Fig. 8.** Best-fit linear relationship between 10'aDRI and aDRI indices of other recording intervals.  
42  
43 18  
44  
45  
46

47 19 In turn, Fig. 9 presents the simple linear regression between the 10'DRWP index and the DRWP values  
48  
49 20 associated with other recording intervals, for the 6 stations analysed. Given the absence of specific studies  
50  
51 21 on the DRWP exposure variable, in this case, it is not possible to compare the similarity between  
52  
53 22 adjustments obtained in different geographic regions, not even between DRWP values based on datasets  
54  
55 23 with low time resolution).  
56  
57  
58  
59  
60  
61  
62  
63  
64  
65

1  
2  
3 1 However, it is observed in Fig. 9 that the coefficients of determination identified for these weather  
4  
5 2 stations are similar to those of the aDRI indices, surpassing 0.97 for the 10'DRWP-hDRWP and  
6  
7 3 10'DRWP-dDRWP adjustments. As expected, this  $R^2$  coefficient increases in both exposure parameters  
8  
9 4 by reducing the recording interval considered.

10  
11  
12  
13 5 On the other hand, several previous studies have found strong correlations between the wind pressure of  
14  
15 6 the location and the value of DRWP in places as diverse as Chile, Brazil and Spain itself [24, 26, 38],  
16  
17 7 reflecting the linkage of the DRWP value to the wind conditions of each site. Again, additional studies in  
18  
19 8 other geographical areas will be necessary to verify that the proposed DRWP extrapolations can be used  
20  
21 9 in regions with similar climatic conditions to those of this study.  
22  
23  
24

25 10  
26  
27  
28 11 **Fig. 9.** Best-fit linear relationship between 10'DRWP and DRWP indices of other recording intervals.  
29  
30  
31  
32

#### 33 34 13 **4. Conclusions**

35  
36  
37 14 This manuscript analyses the effect of the time resolution of climate records on the accuracy of the semi-  
38  
39 15 empirical scalar indices that characterise WDR and DRWP exposures. For this purpose, long series of 10-  
40  
41 16 min, daily, monthly and annual records gathered at sites subject to different exposures and conditions  
42  
43 17 have been used. Taking exhaustive 10-min records as a reference, this error analysis provides a broad  
44  
45 18 perspective on the nature and magnitude of the uncertainties associated with each possible recording  
46  
47 19 interval.  
48  
49

50  
51  
52 20 The results indicate that the main source of error for the calculation of aDRI indices corresponds to the  
53  
54 21 use of wind velocity records that are not simultaneous to precipitation events (co-occurrence error).  
55

56 22 However, the error due to the average of the meteorological variables in longer intervals is more  
57  
58 23 significant for the DRWP calculation.  
59  
60  
61  
62  
63  
64  
65

1  
2  
3  
4  
5  
6  
7  
8  
9  
10  
11  
12  
13  
14  
15  
16  
17  
18  
19  
20  
21  
22  
23  
24  
25  
26  
27  
28  
29  
30  
31  
32  
33  
34  
35  
36  
37  
38  
39  
40  
41  
42  
43  
44  
45  
46  
47  
48  
49  
50  
51  
52  
53  
54  
55  
56  
57  
58  
59  
60  
61  
62  
63  
64  
65

1 In general, the error is reduced by using climate records with a better time resolution. However, DRWP  
2 indices present greater sensitivity to the time resolution of the dataset, requiring more exhaustive  
3 recording intervals to reduce their uncertainty range. Thus, the hourly and daily datasets may be  
4 considered sufficiently accurate to characterise the scalar WDR and DRWP exposures, respectively (with  
5 errors less than 11%). On the contrary, the monthly and annual climate records (in addition to the daily  
6 records for the calculation of the DRWP exposure) should be discarded, owing to their high uncertainty.  
7 The results provided can be used as a guide to reinterpret scalar exposures already obtained through low-  
8 resolution datasets, in addition to estimate the uncertainty of future results in which the available climate  
9 data do not reach the required quality.

10 In any case, fitting relationships capable of extrapolating accurate values of aDRI and DRWP (similar to  
11 those based on 10-min records), from low-resolution datasets have also been presented. The  
12 representativeness of the study conditions and their comparison with results obtained in other regions and  
13 climates suggest that these relationships can be useful in other places with similar climatic conditions.  
14 Nevertheless, it is still necessary to validate and refine these extrapolations, which opens a new and  
15 interesting line of work for the study of raw meteorological data in different regions of the world.

16  
17 **Acknowledgements**

18 This work was partially financed by the Spanish Ministry of Science and Innovation and the FICYT co-  
19 financed with FEDER funds under the Research Projects BIA2012-31609 and FC-15-GRUPIN14-004.

20 **References**

21 [1] Basheer PAM, Long AE, Montgomery FR. An interaction model for causes of deterioration of concrete. In,  
22 Malhotra Symposium on Concrete Technology. San Francisco: American Concrete Institute; 1994, p. 213-33.

1  
2  
3  
4  
5  
6  
7  
8  
9  
10  
11  
12  
13  
14  
15  
16  
17  
18  
19  
20  
21  
22  
23  
24  
25  
26  
27  
28  
29  
30  
31  
32  
33  
34  
35  
36  
37  
38  
39  
40  
41  
42  
43  
44  
45  
46  
47  
48  
49  
50  
51  
52  
53  
54  
55  
56  
57  
58  
59  
60  
61  
62  
63  
64  
65

1 [2] Tang W, Davidson CI, Finger S, Vance K. Erosion of limestone building surfaces caused by wind-driven rain.  
2  
3 1. Field measurements. *Atmos Environ* 2004; 38(33): 5589-99.  
4  
5 2  
6  
7 3 <http://dx.doi.org/10.1016/j.atmosenv.2004.06.030>.  
8  
9  
10 4 [3] Hall C, Hoff WD. *Water transport in brick, stone and concrete*. 2nd ed. New York: Spon Press.; 2012.  
11  
12  
13 5 [4] Erkal A, D'Ayala D, Sequeira L. Assessment of wind-driven rain impact, related surface erosion and surface  
14  
15 6 strength reduction of historic building materials. *Build Environ* 2012; 57:336-48.  
16  
17 7 <http://dx.doi.org/10.1016/j.buildenv.2012.05.004>.  
18  
19  
20 8 [5] D'ayala D, Aktas YD. Moisture dynamics in the masonry fabric of historic buildings subjected to wind-driven  
21  
22 9 rain and flooding. *Build Environ* 2016; 104(1):208-220. <http://dx.doi.org/10.1016/j.buildenv.2016.05.015>.  
23  
24  
25 10 [6] Abuku M, Blocken B, Roels S. Moisture response of building facades to wind-driven rain: Field measurements  
26  
27 11 compared with numerical simulations. *J Wind Eng Ind Aerod* 2009; 97(5-6):197-207.  
28  
29 12 <http://dx.doi.org/10.1016/j.jweia.2009.06.006>.  
30  
31  
32 13 [7] Abuku M, Janssen H, Roels S. Impact of wind-driven rain on historic brick wall buildings in a moderately cold  
33  
34 14 and humid climate: Numerical analyses of mould growth risk, indoor climate and energy consumption. *Energ*  
35  
36 15 *Buildings* 2009; 41(1):101-10. <http://dx.doi.org/10.1016/j.enbuild.2008.07.011>.  
37  
38  
39 16 [8] Nascimento MLM, Bauer E, de Souza JS, Zanoni VAG. Wind-driven rain incidence parameters obtained by  
40  
41 17 hygrothermal simulation. *J Build Rehabil* 2016; 1-5. <http://dx.doi.org/10.1007/s41024-016-0006-5>.  
42  
43  
44 18 [9] WHO. Environmental burden of disease associated with inadequate housing. Methods for quantifying health  
45  
46 19 impacts of selected housing risks in the WHO European region. Copenhagen: World Health Organization;  
47  
48 20 2011.  
49  
50  
51 21 [10] Sahal AN, Lacasse MA. Experimental assessment of water penetration and entry into siding-clad wall  
52  
53 22 specimen (Internal Report No. 862). Ottawa: Institute for Research in Construction, National Research Council  
54  
55 23 Canada; 2004.  
56  
57  
58  
59  
60  
61  
62  
63  
64  
65

1  
2  
3  
4  
5  
6  
7  
8  
9  
10  
11  
12  
13  
14  
15  
16  
17  
18  
19  
20  
21  
22  
23  
24  
25  
26  
27  
28  
29  
30  
31  
32  
33  
34  
35  
36  
37  
38  
39  
40  
41  
42  
43  
44  
45  
46  
47  
48  
49  
50  
51  
52  
53  
54  
55  
56  
57  
58  
59  
60  
61  
62  
63  
64  
65

1 [11] Cornick SM, Lacasse MA. A review of climate loads relevant to assessing the watertightness performance of  
2 walls, windows, and wall-window interfaces. *J ASTM Int* 2005; 2(10):1-16.  
3 <http://dx.doi.org/10.1520/JAI12505>.  
4  
5 [12] Blocken B, Derome J, Carmeliet J. Rainwater runoff from building facades: A review. *Build Environ* 2013;  
6 60:339-61. <http://dx.doi.org/10.1016/j.buildenv.2012.10.008>.  
7  
8 [13] Lacy RE, Shellard HC. An index of driving rain. *Meteorol Mag* 1962; 91(1080):177-84.  
9  
10 [14] Straube JF, Burnett EFP. Simplified prediction of driving rain deposition. In: *Proceedings of International*  
11 *Building Physics Conference*. Eindhoven; 2000, p. 375-82.  
12  
13 [15] Blocken B, Carmeliet, J. A review of wind-driven rain research in building science. *J Wind Eng Ind Aerodyn*  
14 2004; 92(13):1079-130. <http://dx.doi.org/10.1016/j.jweia.2004.06.003>.  
15  
16 [16] ANSI/ASHRAE Standard 160. *Criteria for moisture-control design analysis in buildings*. American Society of  
17 *Heating and Air-Conditioning Engineers*, Atlanta; 2009.  
18  
19 [17] EN ISO 15927-3. *Hygrothermal performance of buildings. Calculation and presentation of climatic data. Part 3:*  
20 *calculation of a driving rain index for vertical surfaces from hourly wind and rain data*. European Committee  
21 *for Standardization*; 2009.  
22  
23 [18] Lacasse MA, O'Connor T, Nunes SC, Beaulieu P. (2003). *Report from Task 6 of MEWS Project:*  
24 *Experimental assessment of water penetration and entry into wood-frame wall specimens – Final Report*  
25 *(Institute for Research in Construction - Internal Report 113)*. Ottawa: National Research Council Canada;  
26 2003.  
27  
28 [19] EN 12865. *Hygrothermal performance of building components and building elements. Determination of the*  
29 *resistance of external wall systems to driving rain under pulsating air pressure*. European Committee for  
30 *Standardization*; 2001.  
31  
32 [20] AAMA 501.1. *Standard test method for water penetration of exterior windows, curtain walls and doors using*  
33 *dynamic pressure*. American Architectural Manufacturers Association; 2005.

1  
2  
3  
4  
5  
6  
7  
8  
9  
10  
11  
12  
13  
14  
15  
16  
17  
18  
19  
20  
21  
22  
23  
24  
25  
26  
27  
28  
29  
30  
31  
32  
33  
34  
35  
36  
37  
38  
39  
40  
41  
42  
43  
44  
45  
46  
47  
48  
49  
50  
51  
52  
53  
54  
55  
56  
57  
58  
59  
60  
61  
62  
63  
64  
65

1 [21] ASTM E311-00. Standard test method for water penetration of exterior windows, skylights, doors, and curtain  
2 walls by uniform static air pressure difference. American Society for Testing and Materials; 2009.

3 [22] Welsh RE, Skinner WR, Morris RJ. A climatology of driving rain pressure for Canada (Climate and  
4 Atmospheric Research Directorate Draft Report). Gatineau: Environment Canada, Atmospheric Environment  
5 Service; 1989.

6 [23] Pérez JM, Domínguez J, Rodríguez B, del Coz JJ, Cano E. Combined use of wind-driven rain and wind  
7 pressure to define water penetration risk into building façades: The Spanish case. *Build Environ* 2013; 64:46-  
8 56. <http://dx.doi.org/10.1016/j.buildenv.2013.03.004>.

9 [24] Pérez JM, Domínguez J, Cano E, del Coz JJ, Martín A. Procedure for a detailed territorial assessment of wind-  
10 driven rain and driving-rain wind pressure and its implementation to three Spanish regions. *J Wind Eng Ind  
11 Aerodyn* 2014; 128:76-89. <http://dx.doi.org/10.1016/j.jweia.2014.02.008>.

12 [25] Blocken B, Carmeliet J. On the validity of the cosine projection in wind-driven rain calculations on buildings.  
13 *Build Environ* 2006; 41(9):1182-9. <http://dx.doi.org/10.1016/j.buildenv.2005.05.002>.

14 [26] Pérez JM, Domínguez J, Cano E, del Coz JJ, Alonso M. Global analysis of building façade exposure to water  
15 penetration in Chile. *Build Environ* 2013; 70:284-297. <http://dx.doi.org/10.1016/j.buildenv.2013.09.001>.

16 [27] WMO. Guide to Meteorological Instruments and Methods of Observation. WMO-No 8. Geneva: World  
17 Meteorological Organization; 2008.

18 [28] Skerlj PF. A Critical assessment of the driving rain wind pressures used in CSA Standard CAN/CSA-A44-M90.  
19 M.A.Sc. Thesis, Faculty of Engineering Science, University of Western Ontario, London, Canada; 1999.

20 [29] Blocken B, Carmeliet J. On the errors associated with the use of hourly data in wind-driven rain calculations on  
21 building facades. *Atmos Environ* 2007; 41:2335-43. <http://dx.doi.org/10.1016/j.atmosenv.2006.11.014>.

22 [30] Blocken B, Carmeliet J. Guidelines for the required time resolution of meteorological input data for wind-  
23 driven rain calculations on buildings. *J Wind Eng Ind Aerodyn* 2008; 96:621-39.  
24 <http://dx.doi.org/10.1016/j.jweia.2008.02.008>.

1  
2  
3  
4  
5  
6  
7  
8  
9  
10  
11  
12  
13  
14  
15  
16  
17  
18  
19  
20  
21  
22  
23  
24  
25  
26  
27  
28  
29  
30  
31  
32  
33  
34  
35  
36  
37  
38  
39  
40  
41  
42  
43  
44  
45  
46  
47  
48  
49  
50  
51  
52  
53  
54  
55  
56  
57  
58  
59  
60  
61  
62  
63  
64  
65

1 [31] Pérez JM, Domínguez J, Rodríguez B, del Coz JJ, Cano E. Estimation of the exposure of buildings to driving  
2 rain in Spain from daily wind and rain data. *Build Environ* 2012; 57:259-70.  
3 <http://dx.doi.org/10.1016/j.buildenv.2012.05.010>  
4  
5 [32] Ge H. Influence of time resolution and averaging techniques of meteorological data on the estimation of wind-  
6 driven rain load on building facades for Canadian climates. *J Wind Eng Ind Aerodyn* 2015; 143:50-61.  
7 <http://dx.doi.org/10.1016/j.jweia.2015.04.019>.  
8  
9 [33] Hoppestad S. Slagregninorge (Driving rain in Norway, in Norwegian). Norwegian Building Research Institute  
10 Report no. 13.Oslo: NBI; 1955.  
11  
12 [34] Cornick SM, Dalglish A, Said N, Djebbar R, Tariku F, Kumaran MK. Report from Task 4 of MEWS Project:  
13 Task 4 – Environmental conditions final report (Research Report No. 113). Ottawa: National Research Council  
14 Canada; 2002.  
15  
16 [35] Giarma C, Aravantinos D. Estimation of building components' exposure to moisture in Greece based on wind  
17 rainfall and other climatic data. *J Wind Eng Ind Aerodyn* 2011; 99:91-102.  
18 <http://dx.doi.org/10.1016/j.jweia.2010.12.001>.  
19  
20 [36] Akingbade FOA. Estimation of driving rain index for Nigeria. *Archit Sci Rev* 2004; 47(2):103-106.  
21 <http://dx.doi.org/10.1080/00038628.2004.9697032>.  
22  
23 [37] Chand I, Bhargava PK. Estimation of driving rain index for India. *Build Environ* 2002; 37(5):549-554.  
24 [http://dx.doi.org/10.1016/S0360-1323\(01\)00057-9](http://dx.doi.org/10.1016/S0360-1323(01)00057-9)  
25  
26 [38] Domínguez J, Pérez JM, Alonso M, Cano E, del Coz JJ. Assessment of water penetration risk in building  
27 facades throughout Brazil. *Build Res Inf* 2016; In press. <http://dx.doi.org/10.1080/09613218.2016.1183441>.  
28  
29 [39] Van der Hoven I. Power spectrum of horizontal wind speed in the frequency range from 0.0007-900 cycles  
30 per hour. *J Meteorol* 1957; 14:160-4. [http://dx.doi.org/10.1175/1520-0469\(1957\)014<0160:PSOHWS>2.0.CO;2](http://dx.doi.org/10.1175/1520-0469(1957)014<0160:PSOHWS>2.0.CO;2).

1  
2  
3  
4  
5  
6  
7  
8  
9  
10  
11  
12  
13  
14  
15  
16  
17  
18  
19  
20  
21  
22  
23  
24  
25  
26  
27  
28  
29  
30  
31  
32  
33  
34  
35  
36  
37  
38  
39  
40  
41  
42  
43  
44  
45  
46  
47  
48  
49  
50  
51  
52  
53  
54  
55  
56  
57  
58  
59  
60  
61  
62  
63  
64  
65

1 [40] Jones DMA, Sims AL. Climatology of instantaneous rainfall rates. *J Appl Meteorol* 1978; 17:1135-50.  
2  
3  
4  
5 2 [http://dx.doi.org/10.1175/1520-0450\(1978\)017<1135:COIRR>2.0.CO;2](http://dx.doi.org/10.1175/1520-0450(1978)017<1135:COIRR>2.0.CO;2).  
6  
7  
8 3 [41] Sumner G. *Precipitation: Process and analysis*. New York: John Wiley & Sons; 1988.  
9  
10  
11 4 [42] Giarma C, Aravantinos D. On building components' exposure to driving rain in Greece. *J Wind Eng Ind*  
12  
13 5 *Aerodyn* 2014; 125:133-145. <http://dx.doi.org/10.1016/j.jweia.2013.11.014>.  
14  
15  
16 6 [43] Xunta of Galicia. Department of Environment, Territory and Infrastructures. Galicia, Spain.  
17  
18 7 <http://www.meteogalicia.gal/> [Last accessed 19.05.2017].  
19  
20  
21 8 [44] Kottek M, Grieser J, Beck C, Rudolf B, Rubel F. World map of the Köppen-Geiger climate classification  
22  
23 9 updated. *Meteorol Z* 2006; 15:259-63. <http://dx.doi.org/10.1127/0941-2948/2006/0130>.  
24  
25  
26  
27  
28  
29  
30  
31  
32  
33  
34  
35  
36  
37  
38  
39  
40  
41  
42  
43  
44  
45  
46  
47  
48  
49  
50  
51  
52  
53  
54  
55  
56  
57  
58  
59  
60  
61  
62  
63  
64  
65

## Highlights

- Study of 10-min, hourly, daily, monthly and annually climate data, over 15 years
- Scalar calculation of WDR and DRWP exposure indices in Spanish locations
- Significance of the dataset recording interval on the accuracy of these indices
- Magnitude of the error sources associated with each possible recording interval
- Mathematical correlations for estimate the WDR and DRWP exposures

## List of tables

**Table 1.** Exposure results to wind-driven rain and simultaneous wind pressure for climate datasets of different time resolution.

**Table 2.** Exposure results without co-occurrence error for climate datasets with different time resolutions.

**Table 3.** Percentage errors derived from the non-co-occurrence of wind and rain ( $e_1$ ) and from the averaged data ( $e_2$ ) for climate datasets of different time resolution (regarding 10-min values).

**Table 1.**

Exposure results to wind-driven rain and simultaneous wind pressure for climate datasets of different time resolution.

aDRI (m <sup>2</sup> /s)	CIS Ferrol	Pedro Murias	Corrubedo	Campus Lugo	Quimadelos	O Invernadeiro
<b>10'aDRI</b>	<b>5.02</b>	<b>3.66</b>	<b>7.98</b>	<b>2.23</b>	<b>4.07</b>	<b>5.39</b>
<b>haDRI</b>	4.86	3.59	7.99	2.18	4.05	5.36
<b>daDRI</b>	4.76	3.59	7.00	2.06	3.62	4.83
<b>maDRI</b>	4.00	2.93	4.60	1.67	2.65	3.74
<b>aaDRI</b>	3.97	2.71	4.07	1.71	2.50	3.61

DRWP (Pa)	CIS Ferrol	Pedro Murias	Corrubedo	Campus Lugo	Quimadelos	O Invernadeiro
<b>10'DRWP</b>	<b>11.41</b>	<b>11.10</b>	<b>40.82</b>	<b>4.20</b>	<b>3.57</b>	<b>8.02</b>
<b>hDRWP</b>	10.61	10.84	35.90	3.63	3.00	7.06
<b>dDRWP</b>	8.29	8.67	22.04	2.56	1.84	4.56
<b>mDRWP</b>	6.11	5.51	10.83	1.99	1.24	3.24
<b>aDRWP</b>	5.96	5.19	10.18	1.92	1.20	3.19

**Table 2.**

Exposure results without co-occurrence error for climate datasets with different time resolutions.

$aDRI_{e2}$ ( $m^2/s$ )	CIS Ferrol	Pedro Murias	Corrubedo	Campus Lugo	Quimadelos	O Invernadeiro
<b>10'aDRI</b>	<b>5.02</b>	<b>3.66</b>	<b>7.98</b>	<b>2.23</b>	<b>4.07</b>	<b>5.39</b>
<b>haDRI<sub>e2</sub></b>	4.97	3.63	8.05	2.22	4.08	5.40
<b>daDRI<sub>e2</sub></b>	4.97	3.60	7.93	2.17	3.99	5.30
<b>maDRI<sub>e2</sub></b>	4.66	3.52	7.63	2.06	3.80	5.06
<b>aaDRI<sub>e2</sub></b>	4.61	3.50	7.56	2.06	3.80	5.01
DRWP <sub>e2</sub> (Pa)	CIS Ferrol	Pedro Murias	Corrubedo	Campus Lugo	Quimadelos	O Invernadeiro
<b>10'DRWP</b>	<b>11.41</b>	<b>11.10</b>	<b>40.82</b>	<b>4.20</b>	<b>3.57</b>	<b>8.02</b>
<b>hDRWP<sub>e2</sub></b>	11.54	11.53	37.18	3.89	3.15	7.35
<b>dDRWP<sub>e2</sub></b>	9.49	9.99	28.36	2.85	2.28	5.10
<b>mDRWP<sub>e2</sub></b>	7.74	7.20	27.27	2.67	2.35	5.09
<b>aDRWP<sub>e2</sub></b>	8.08	7.50	30.81	2.83	2.78	5.53

**Table 3.**

Percentage errors derived from the non-co-occurrence of wind and rain ( $e_1$ ) and from the averaged data ( $e_2$ ) for climate datasets of different time resolution (regarding 10-min values).

	haDRI			daDRI			maDRI			aaDRI		
	$e_1$	$e_2$	$e_1+e_2$									
<b>CIS Ferrol</b>	-2.2	-0.9	-3.1	-4.3	-0.9	-5.2	-13.1	-7.2	-20.9	-12.7	-8.2	-20.9
<b>Pedro Murias</b>	-1.2	-0.7	-1.9	-0.2	-1.6	-1.8	-16.0	-3.9	-19.8	-21.6	-4.3	-25.9
<b>Corrubedo</b>	-0.7	+0.8	+0.1	-11.7	-0.6	-12.3	-38.0	-4.4	-42.3	-43.8	-5.2	-49.0
<b>Campus Lugo</b>	-1.9	-0.7	-2.5	-5.0	-2.9	-7.9	-17.8	-7.6	-25.4	-16.1	-7.6	-23.6
<b>Queimadelos</b>	-0.9	+0.3	-0.7	-9.2	-2.1	-11.2	-28.3	-6.6	-34.9	-31.8	-6.8	-38.6
<b>O Invernadeiro</b>	-0.7	+0.3	-0.4	-8.8	-1.7	-10.4	-24.4	-6.1	-30.6	-25.9	-7.1	-33.0
	hDRWP			dDRWP			mDRWP			aDRWP		
	$e_1$	$e_2$	$e_1+e_2$									
<b>CIS Ferrol</b>	-8.2	+1.1	-7.0	-10.5	-16.9	-27.4	-14.3	-32.1	-46.5	-18.6	-29.2	-47.8
<b>Pedro Murias</b>	-6.2	+3.8	-2.3	-11.8	-10.0	-21.9	-15.2	-35.1	-50.4	-20.8	-32.4	-53.3
<b>Corrubedo</b>	-3.1	-8.9	-12.0	-15.5	-30.5	-46.0	-40.3	-33.2	-73.5	-50.6	-24.5	-75.1
<b>Campus Lugo</b>	-6.4	-7.2	-13.5	-6.7	-32.2	-38.9	-16.2	-36.3	-52.5	-21.6	-32.7	-54.3
<b>Queimadelos</b>	-4.3	-11.6	-15.9	-12.4	-36.0	-48.4	-30.9	-34.2	-65.1	-44.1	-22.2	-66.2
<b>O Invernadeiro</b>	-3.6	-8.4	-12.0	-6.8	-36.4	-43.2	-23.0	-36.6	-59.6	-29.2	-31.0	-60.2

## Figure captions

**Fig. 1.** Characteristics and location of the 6 analysed weather stations.

**Fig. 2.** Location of the 6 weather stations selected for the conducted study. *Darker colours represent higher elevations.*

**Fig. 3.** Magnitude and nature of the aDRI error associated with each recording interval and its fluctuation for the different analysed locations.

**Fig. 4.** Magnitude and nature of the DRWP error associated with each recording interval and its fluctuation for the different analysed locations.

**Fig. 5.** Evolution of mean calculation errors in aDRI values for the usual recording intervals used for climate datasets (logarithmic scale).

**Fig. 6.** Evolution of mean calculation errors in DRWP values for the usual recording intervals used for climate datasets (logarithmic scale).

**Fig. 7.** (a) Best-fit linear relationship between daDRI and maDRI; (b) best fit-linear relationship between daDRI and aaDRI, and its comparison with different countries.

**Fig. 8.** Best-fit linear relationship between  $10^4$ aDRI and aDRI indices of other recording intervals.

**Fig. 9.** Best-fit linear relationship between  $10^4$ DRWP and DRWP indices of other recording intervals.



**CIS Ferrol**  
 (Ferrol city municipality)  
 Coastal zone / drowned river valley  
 Altitude: 37 m  
 Rain gauge: R.M.Young 52202/03  
 Average rainfall: 1,257 mm/year  
 Anemometer: Ornytion 107H4M  
 Mean wind velocity: 3.14 m/s  
 Missing data: 0.98%



**Pedro Murias**  
 (Ribadeo municipality)  
 Coastal zone / drowned river valley  
 Altitude: 51 m  
 Rain gauge: R.M.Young 52202/03  
 Average rainfall: 986 mm/year  
 Anemometer: Ornytion 107U  
 Mean wind velocity: 2.94 m/s  
 Missing data: 0.65%



**Corrubedo**  
 (Ribeira municipality)  
 Coastal zone  
 Altitude: 30 m  
 Rain gauge: R.M.Young 52202/03  
 Average rainfall: 1,056 mm/year  
 Anemometer: R.M.Young 05106 MA  
 Mean wind velocity: 4.09 m/s  
 Missing data: 1.22%



**Campus Lugo**  
 (Lugo city municipality)  
 Inland / urban environment  
 Altitude: 400 m  
 Rain gauge: Campbell ARG100  
 Average rainfall: 948 mm/year  
 Anemometer: Ornytion 107U  
 Mean wind velocity: 1.79 m/s  
 Missing data: 0.57%



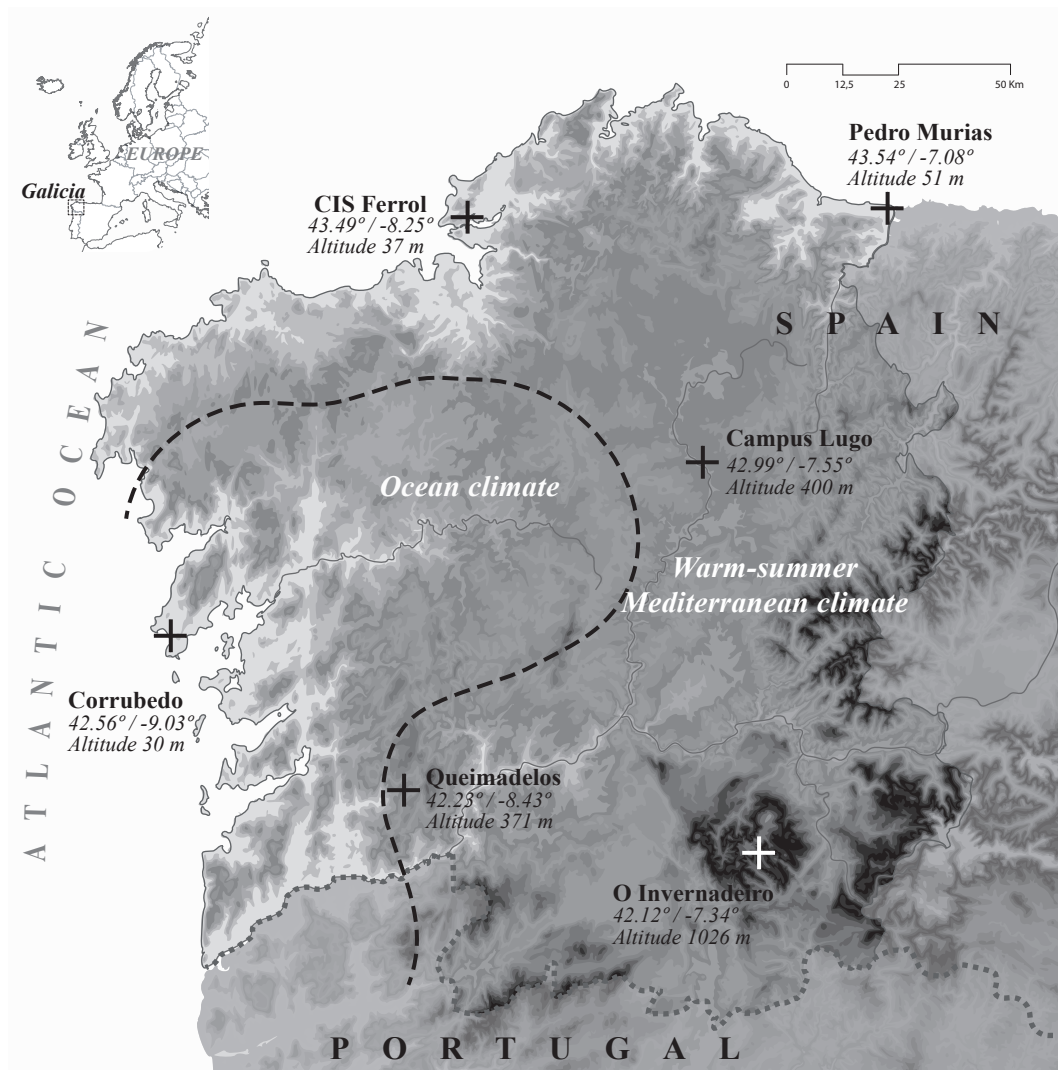
**Queimadelos**  
 (Mondariz municipality)  
 Forest zone  
 Altitude: 371 m  
 Rain gauge: Campbell ARG100  
 Average rainfall: 1,785 mm/year  
 Anemometer: Ornytion 107H/4  
 Mean wind velocity: 1.37 m/s  
 Missing data: 0.46%



**O Invernadeiro**  
 (Vilariño de Conso municipality)  
 Inland / mountain zone  
 Altitude: 1026 m  
 Rain gauge: Thies 5.4032.35.007  
 Average rainfall: 1,651 mm/year  
 Anemometer: Ornytion 107U  
 Mean wind velocity: 2.30 m/s  
 Missing data: 1.50%

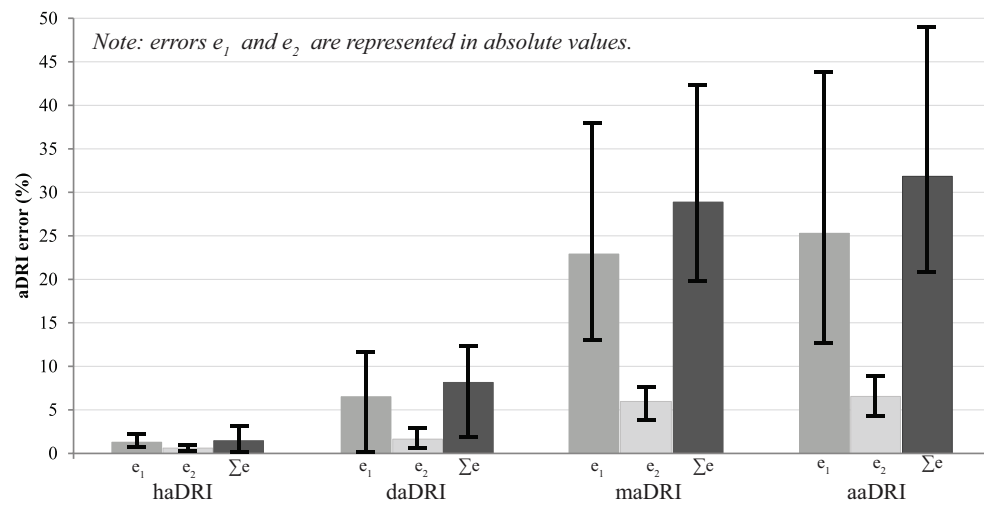
**Fig. 1.** Characteristics and location of the 6 analysed weather stations.

Figure 2



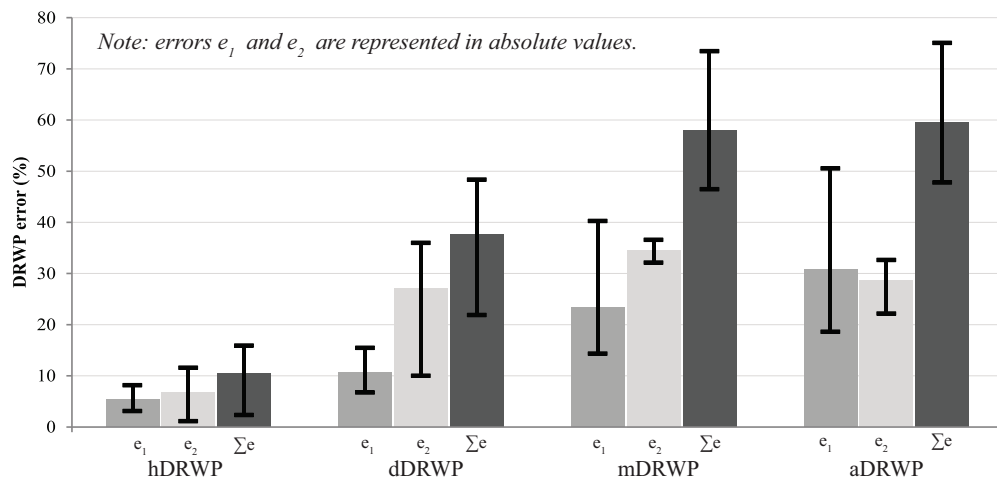
**Fig. 2.** Location of the 6 weather stations selected for the conducted study.  
*Darker colours represent higher elevations.*

Figure 3



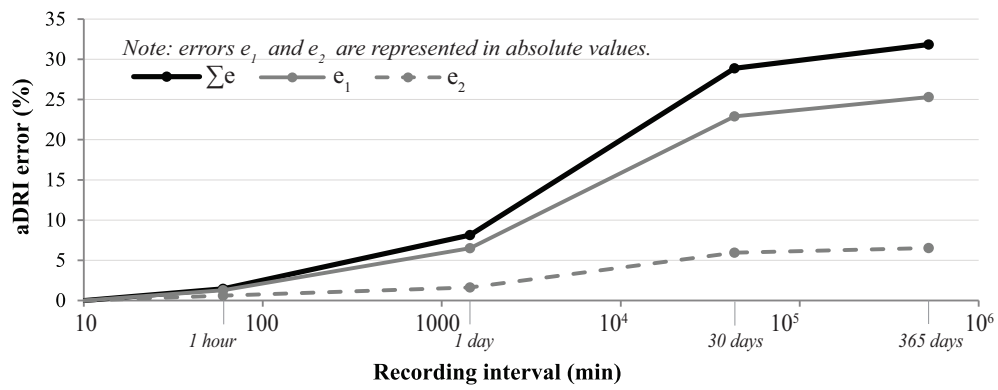
**Fig. 3.** Magnitude and nature of the aDRI error associated with each redording interval and its fluctuation for the different analysed locations.

Figure 4



**Fig. 4.** Magnitude and nature of the DRWP error associated with each redording interval and its fluctuation for the different analysed locations.

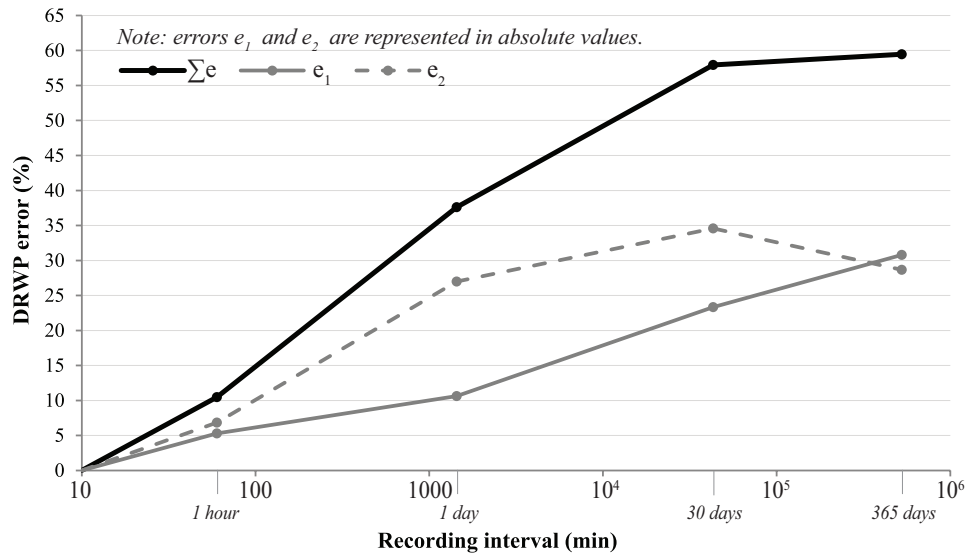
Figure 5



(%)	Hourly dataset	Daily dataset	Monthly dataset	Annual dataset
Total mean error	1.46	8.15	28.87	31.83
Standard deviation	1.2	4.0	8.8	10.6
Mean error $e_1$	1.28	6.51	22.91	25.30
Standard deviation	0.6	4.2	9.3	11.3
Mean error $e_2$	0.61	1.64	5.96	6.54
Standard deviation	0.3	0.8	1.5	1.5

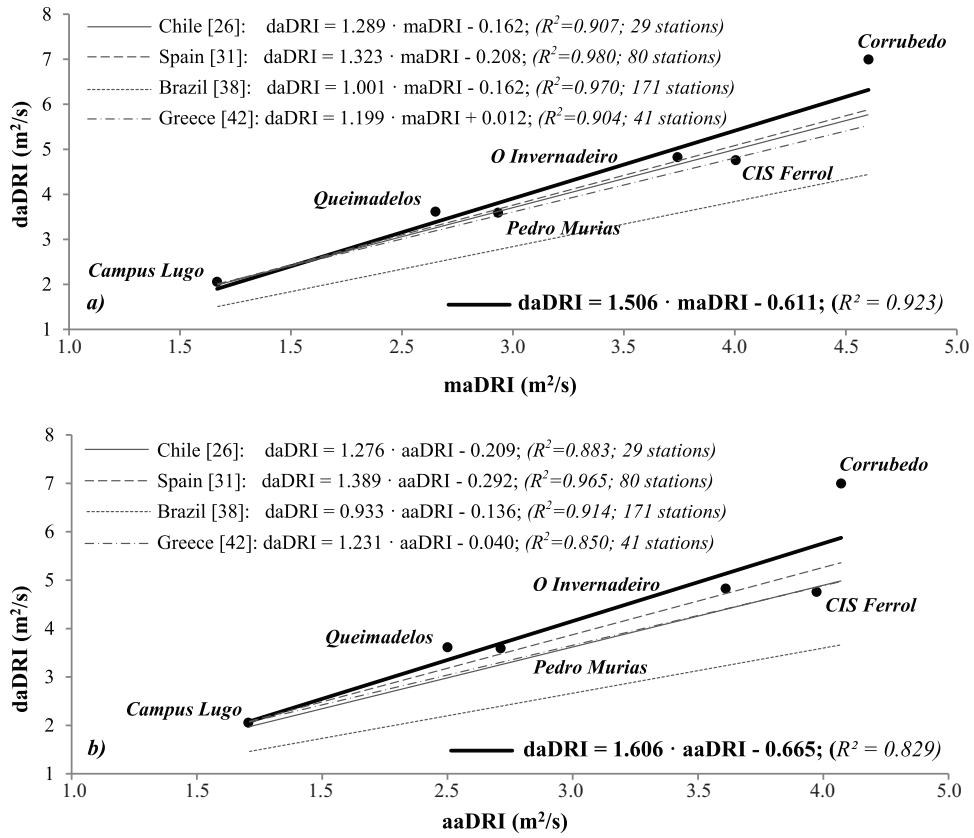
Fig. 5. Evolution of mean calculation errors in aDRI values for the usual recording intervals used for climate datasets (logarithmic scale).

Figure 6



(%)	Hourly dataset	Daily dataset	Monthly dataset	Annual dataset
Total mean error	10.48	37.62	57.92	59.47
Standard deviation	4.9	10.7	10.1	9.9
Mean error $e_1$	5.29	10.62	23.33	30.81
Standard deviation	1.9	3.4	10.4	13.4
Mean error $e_2$	6.85	27.00	34.59	28.66
Standard deviation	3.8	10.9	1.7	4.4

Fig. 6. Evolution of mean calculation errors in DRWP values for the usual recording intervals used for climate datasets (logarithmic scale).



**Fig. 7.** a) Best-fit linear relationship between daDRI and maDRI; b) best fit-linear relationship between daDRI and aaDRI, and its comparison with different countries.

Figure 8

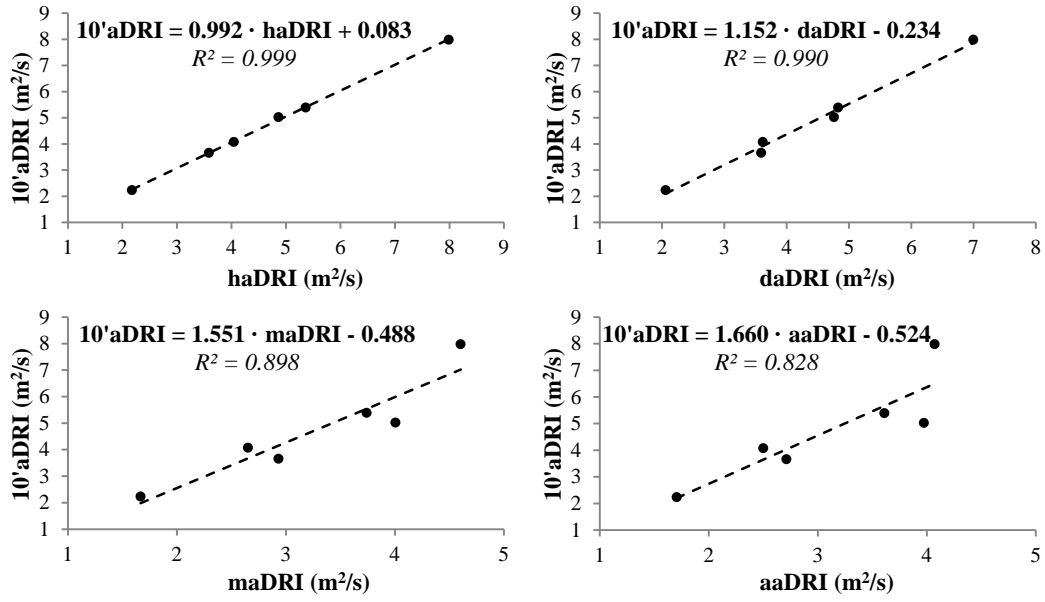


Fig. 8. Best-fit linear relationship between  $10'aDRI$  and aDRI indices of other recording intervals.

Figure 9

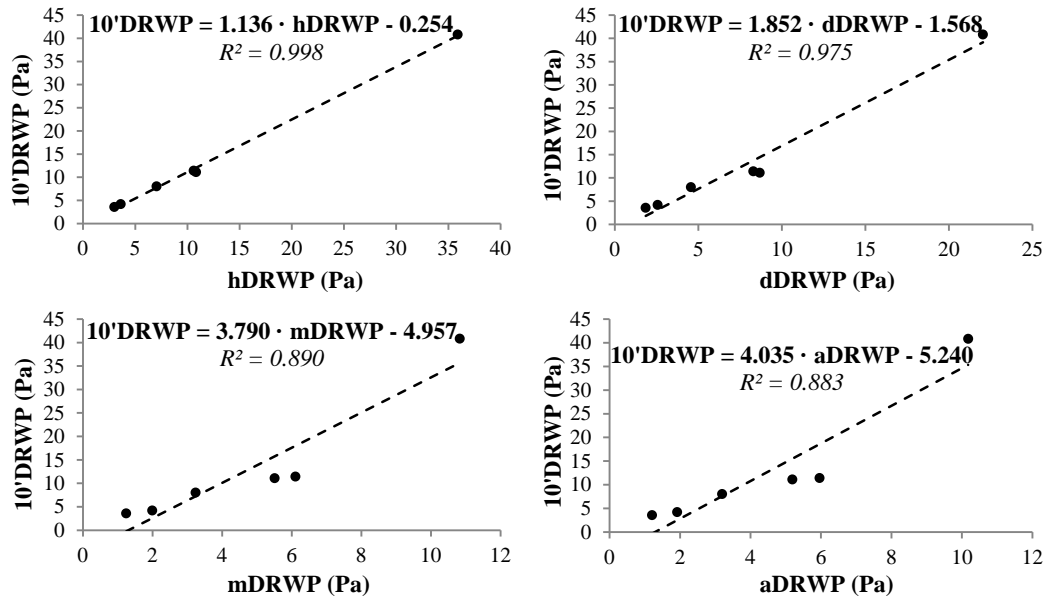


Fig. 9. Best-fit linear relationship between 10' DRWP and DRWP indices of other recording intervals.